pendent behavior. For sufficiently large applied fields, it is possible for canting of the Fe^{2+} and Fe^{3+} sublattice moments to occur. However, the high critical temperature of the present system and concomitant strong intersublattice exchange interaction suggest that such canting will be negligible and not observable in the powder Mössbauer spectra.

To conclude it is worthwhile to compare some of our low-temperature results with those for the higher hydrate $Fe_2F_5 \cdot 7H_2O$. This material orders at $T < 3$ K and the details of its zero-field Mössbauer spectrum at 1.3 K have been discussed.[26] In contrast to the dihydrate there appear to be two slightly different but nearly equally populated ferric sites for which H_n = 561 and 573 kG. The effective field at the ferrous sites of $Fe_2F_5 \cdot 7H_2O$ is 146 kG at 1.3 K and is much larger than that observed (41 kG) for the ferrous sites of the dihydrate. The considerable difference in the critical temperatures of these materials, 48.0 K for the dihydrate vs. <3 K for the heptahydrate, suggests that the former must be magnetically more condensed owing to extensive bridging. This is consistent with the proposed discrete ion $[Fe(H_2O)_6^{2+}][FeF_5(H_2O)^{2-}]$ structure of the heptahydrate.

Acknowledgment. This work was supported by the Office of Naval Research. We thank Professor William E. Hatfield for the use of the vibrating sample magnetometers, Dr. Peter J. Corvan for experimental assistance, and Dr. James W. Hall for computational assistance. W. M. Reiff acknowledges partial support of the Research Corporation, HEW Grant No. RR 07143, and the NSF Division of Solid State Chemistry, Grant No. DMR-75-13592 A01. He also thanks the Francis Bitter National Magnet Laboratory for use of its high-field Mössbauer facilities and useful discussion with R. B. Frankel and B. Dockum.

Registry No. Fe_2F_5, 12061-94-8.

References and Notes

(1) (a) University of Vermont. Hood Interdisciplinary Fellowship Awardee. (b) University of Vermont. (c) Northeastern University.
(2) G. Brauer and M. Eichner, *Z. Anorg. Allg. Chem.*, **296**, 13 (1958).
(3) M. B. Robin and P. Day, *Adv. Inorg. Chem. Radiochem.*, **10**, 247 (1967).
(4) J. Portier, *Angew. Chem., Int. Ed. Engl.*, **15**, 475 (1976).
(5) E. G. Walton, P. J. Corvan, D. B. Brown, and P. Day, *Inorg. Chem.*, **15**, 1737 (1976).
(6) T. Sakai and T. Tominaga, *Bull. Chem. Soc. Jpn.* **48**, 3168 (1975).
(7) D. B. Brown and E. G. Walton, Abstracts of Papers, 170th National Meeting of the American Chemical Society, Chicago, Ill., Aug 1975.
(8) P. Charpin and Y. Machetau, *C. R. Hebd. Seances Acad. Sci., Ser. B*, **280**, 61 (1975).
(9) K. J. Gallagher and M. R. Ottaway, *J. Chem. Soc., Dalton Trans.*, 987 (1975).
(10) T. Sakai and T. Tominaga, *Radioisotopes*, **23**, 347 (1974).
(11) P. Imbert, G. Jehanns, Y. Macheteau, and F. Varret, *J. Phys. (Paris)*, **37**, 969 (1976).
(12) W. Hall, S. Kim, J. Zubieta, E. G. Walton, and D. B. Brown, *Inorg. Chem.*, **16**, 1884 (1977).
(13) B. N. Figgis and R. S. Nyholm, *J. Chem. Soc.*, 4190 (1958).
(14) Reference 5, Figure 2.
(15) J. A. Dilts, E. G. Walton, and D. B. Brown, unpublished observations.
(16) J. S. Smart, "Molecular Field Theories of Magnetism", W. B. Saunders, Philadelphia, Pa., 1966.
(17) J. S. Smart, *Am. J. Phys.*, **23**, 356 (1955).
(18) J. B. Goodenough, "Magnetism and the Chemical Bond", Wiley-Interscience, New York, N.Y., 1963.
(19) J. Portier, A. Tressand, R. De Pape, and P. Hagenmuller, *C.R. Hebd. Seances Acad. Sci., Ser. C*, **267**, 1711 (1968).
(20) Reference 16, eq 3.19.
(21) T. Sakai and T. Tominaga, *Radiochem. Radioanal. Lett.*, **23**, 329 (1975).
(22) N. N. Greenwood, and T. C. Gibb, "Mössbauer Spectroscopy", Chapman & Hall, London, 1971.
(23) N. N. Greenwood, A. T. Howe, and F. Memil, *J. Chem. Soc. A*, 2218 (1971).
(24) Sakai and Tominaga (ref 10) have produced analyses of $Fe_2F_5 \cdot 2H_2O$ which exhibit a F/Fe ratio of 4.8/2.
(25) J. Van Dongen Torman, R. Jagannathan, and J. M. Trooster, *Hyperfine Interact.*, **1**, 135 (1975).
(26) P. Imbert, Y. Macheteau, and F. Varret, *J. Phys. (Paris)*, **34**, 49 (1973).

Contribution from the Metcalf Research Laboratories, Brown University, Providence, Rhode Island 02912

Proton, Deuteron, Oxygen-17, and Electron Spin Magnetic Resonance of the Trihydroxovanadyl(IV) Ion. Kinetics and Relaxation

WILLIAM C. COPENHAFER and PHILIP H. RIEGER*

Received December 28, 1976 AIC60907F

Deuteron exchange between $VO(OD)_3(D_2O)_2^-$ and solvent water is fast. The rate constant (at 25 °C) and activation parameters—$k = (8.4 \times 10^6)[OD^-]$ s^{-1}, $\Delta H^\ddagger = 40 \pm 2$ kJ mol^{-1}, $\Delta S^\ddagger = 22 \pm 7$ J mol^{-1} K^{-1}—were determined from ^1H NMR line width measurements of 99% D_2O solutions, corrected for nonkinetic relaxation contributions using relaxation times computed from ESR data. A mechanism involving deuteron transfer from an equatorial aquo ligand to hydroxide ion is postulated. ESR line width studies suggest a hydroxo proton hyperfine coupling of about 4.4 G. The ^1H NMR and ESR data were used to predict ^2H NMR line widths which are in good agreement with experimental values. Oxygen exchange between $VO(OH)_3(H_2O)_2^-$ and solvent water is slow on the ^{17}O NMR time scale; a lower limit of 7×10^{-5} s is calculated for the lifetime of an oxygen atom in the first coordination sphere at 65 °C. The experiment was limited by the low solubility of the trihydroxovanadyl ion, ca. 2 mM at 25 °C; the low solubility also precluded measurement of ^1H, ^2H, and ^{17}O contact shifts.

Introduction

Vanadium(IV) has recently been shown to exist in strongly basic aqueous solutions as a trihydroxo complex, $VO(OH)_3(H_2O)_2^-$.[1,2] Analysis of the ESR and optical spectra indicated that the basic solution species was structurally related to the pentaaquovanadyl ion, $VO(H_2O)_5^{2+}$, by the ionization of protons from three equatorial aquo ligands.

Comparison of the optical spectra of the trihydroxo anion and the aquo cation suggested that the equatorial vanadium–oxygen bonds of $VO(OH)_3(H_2O)_2^-$ have more metal character than those of $VO(H_2O)_5^{2+}$. The more covalent character of these bonds might result in slower oxygen exchange with the solvent than was observed for the aquo cation.[3] On the other hand, since both hydroxo and aquo ligands are present at the equatorial coordination sites of $VO(OH)_3(H_2O)_2^-$, electrostatic and trans-effect considerations predict that the rate of oxygen exchange with the solvent might be enhanced. Since both proton donor and proton acceptor sites are available, it was thought that $VO(OH)_3(H_2O)_2^-$ might act as a bifunctional reagent with respect to proton exchange, analogous to $Pt(NH_2)(NH_3)_5^{3+}$[4] and $Cr(OH)(H_2O)_5^{2+}$,[5] which have been shown to undergo very rapid proton exchange with solvent water, presumably by a concerted mechanism involving a cyclic hydrogen-bonded complex which has the

effect of rapidly averaging the proton deficiency among the six ligands.

A surprising feature of the ESR analysis was an indication of an unusually large hyperfine coupling of the vanadium unpaired electron to the equatorial ligand protons. The average coupling of the five equatorial protons was estimated, by analysis of the ESR line widths, at 4.5 G (1.2×10^7 Hz).[2] One of the purposes of the present work was an attempt to confirm this estimate.

In this paper, we report the results of a study of hydrogen and oxygen exchange with the solvent. The investigation follows many of the strategies used by Reuben and Fiat in their work on the aquovanadyl ion.[6]

Experimental Section

Sample Preparation. To avoid air oxidation, all basic solutions of vanadium(IV) were prepared on a vacuum line. Aliquots of a standard NaOH solution and of a $VOSO_4$ (Fisher) solution, standardized by permanganate titration,[7] were placed in separate arms of a Y-shaped tube and degassed by several freeze–pump–thaw cycles. For solutions in D_2O or ^{17}O-enriched water (ca. 7.5%), the water was removed from the solutions under vacuum and the appropriate amount of solvent distilled into the sample tubes. The sample tube assembly was then removed from the vacuum line and the solutions were mixed. For ^1H NMR and ESR samples, the mixed solution was poured into side-arm 5- or 2-mm (o.d.) tubes which were sealed off under vacuum. For ^2H or ^{17}O NMR samples, prepurified nitrogen was added and one of the 8-mm (o.d.) arms of the Y tube used as a sample tube. Samples prepared in this way were stable for several hours as determined by NMR line width measurements.

Viscosity Measurements. The viscosity of 0.1 M NaOH solutions in H_2O and D_2O was measured as a function of temperature with an Ostwald viscometer which had been calibrated with distilled water. Dust was removed from these solutions by passing them through a 15-μm sintered glass filter.

^2H and ^{17}O NMR Spectra. A Varian wide-line NMR spectrometer, equipped with a 12-in. magnet and flux stabilizer, was used in the ^2H and ^{17}O resonance work. Radiofrequency stability at 9.2 MHz (14.1 kG) for ^2H and 7.1 MHz (12.3 kG) for ^{17}O was achieved by locking the Varian V-4210A variable-frequency unit to a frequency synthesizer (Syntest Corp. Model SM-101-70); the frequency was monitored periodically with a HP 524D counter. The sideband method of detection was employed under conditions of high-frequency, low-amplitude field modulation (396 Hz for ^2H, 1500 Hz for ^{17}O). The center band of the first ac component was rejected by detecting in phase with the modulation frequency. Calibration of the spectrum was achieved with an external audio oscillator jacked into the sweep unit at a point after phase detection of the ac component of the resonance signal. Typical line width reproducibility from the average of five spectra was ±5.0%.

The temperature of the samples was controlled with a Varian variable-temperature accessory employing heated or cooled nitrogen and was measured by placing a copper–constantan thermocouple between the sample tube and Dewar walls. In a separate experiment, it was found that the temperature of mineral oil in the sample tube was within 0.5° of the temperature between the sample tube and the Dewar walls if 10–15 min was allowed for equilibration.

^1H NMR Spectra. A Bruker WP-60 spectrometer operating at 60 MHz (14 kG) was used to study the proton resonance of basic solutions of vanadium(IV). Temperature control was achieved with a Varian variable-temperature accessory; the temperature was measured by the method of Van Geet.[8] For each recorded spectrum, ten scans were collected in 8K and averaged with 50-s delays between each scan. The transverse relaxation times were obtained by measuring line widths.

ESR Spectra. A Varian V-4502 ESR spectrometer using 100-kHz field modulation was used to obtain the X-band spectra of vanadium(IV). Temperature control was achieved with a Varian variable-temperature accessory and was measured with a copper–constantan thermocouple. Two spectra were recorded of each solution at each temperature.

Results

^{17}O-NMR Line Width Experiments. Oxygen-17 NMR line widths of 0.1 M NaOH solutions showed the expected temperature dependence (linear in η/T) but exhibited no additional broadening when vanadium(IV) was added. For a 2.0 mM solution of $VO(OH)_3^-$ in aqueous 0.10 M NaOH at 65 °C, the full width at half-height was 76.8 ± 0.6 rad s^{-1}, while for the metal-free hydroxide solution, the width was 77.4 ± 1.1 rad s^{-1} at the same temperature. Because of the limited solubility of $VO(OH)_3^-$, more concentrated solutions could not be prepared. Assuming that an additional broadening of 2 rad s^{-1} could have been observed, a lower limit of 7.2×10^{-5} s is calculated for the lifetime of an oxygen atom in the first coordination sphere of the trihydroxovanadyl ion. This compares with a lifetime of about 6.9×10^{-5} s at 65 °C for the oxygen atoms in the first coordination sphere of the pentaaquo species.[3a] Thus the rate of oxygen exchange in $VO(OH)_3^-$ appears to be at least as slow as that in $VO(H_2O)_5^{2+}$ at 65 °C.

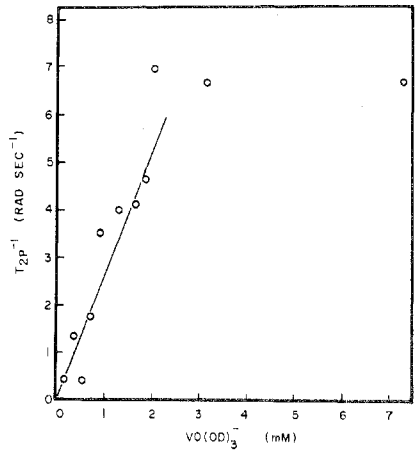

Figure 1. Plot of ^2H NMR line broadening, $1/T_{2p}^D$, vs. concentration of vanadium(IV) in 0.1 M NaOH in D_2O at 25 °C.

Table I. ^2H NMR Line Widths of 0.10 M NaOH in D_2O

t, °C	Obsd width[a]	$T_{2,0}^{-1}$ [a,b]
17.9	10.5 ± 0.5	7.8 ± 0.6
24.3	9.7 ± 0.2	6.8 ± 0.3
30.1	9.2 ± 0.7	6.1 ± 0.9
36.0	8.4 ± 0.4	5.0 ± 0.6
42.8	7.8 ± 0.3	4.2 ± 0.4
48.0	7.6 ± 0.1	3.9 ± 0.1
54.0	7.5 ± 0.3	3.7 ± 0.4
59.8	7.2 ± 0.3	3.3 ± 0.4
66.1	6.8 ± 0.3	2.6 ± 0.4

[a] In units of rad s^{-1}; uncertainties correspond to one standard deviation from the average of five spectra. [b] The calculated Lorentzian contribution to the observed width.

^2H NMR Line Width Experiments. Unlike the ^{17}O resonances, the ^2H NMR spectra of basic solutions containing vanadium(IV) exhibited additional broadening. Figure 1 shows a plot of $T_{2p}^{-1} = T_2^{-1} - T_{2,0}^{-1}$ vs. vanadium(IV) concentration in 0.10 M NaOH at 25 °C for 11 independently prepared samples. Up to about 2 mM, the broadening is linear in vanadium(IV) concentration. Above 2 mM, the residual broadening levels off in a manner reminiscent of the ESR intensity vs. concentration experiment.[1,9] Saturation of $VO(OH)_3^-$ may not be with respect to a precipitate, however. Weiske[10] has interpreted diffusion experiments on basic solutions (pH 10–13) of $Na_2V_3O_7$ ([V(IV)] ≃ 0.04 M) in terms of an oligomer with 12–15 vanadium atoms. A monomer–dodecamer equilibrium (with no species of intermediate size) would account for the results reported here and in ref 1.

Tables I and II list the observed ^2H NMR line width data of 0.10 M NaOH solutions with and without the $VO(OH)_3^-$ species. Figure 2 illustrates that the experimental ^2H NMR line widths of 0.10 M NaOH in D_2O are linear in η/T. The

Table II. ^{2}H NMR Line Width Parameters for 0.92 mM Vanadium(IV) and 0.10 M NaOH in D_2O

t, °C	Obsd width[a]	T_2^{-1} [a,b]	$T_{2,0}^{-1}$ [a,c]	PT_{2p}[d]	T_{2C}^{D} [d,e]
25.5	12.5 ± 0.3	10.1 ± 0.4	6.5 ± 0.3	4.6 ± 0.6	10.4
30.4	13.2 ± 0.4	10.8 ± 0.5	5.8 ± 0.8	3.3 ± 0.6	12.3
35.0	12.5 ± 0.7	10.1 ± 0.8	5.2 ± 0.6	3.4 ± 0.7	14.2
40.0	13.1 ± 0.9	10.7 ± 1.0	4.6 ± 0.4	2.7 ± 0.5	16.2
44.8	13.4 ± 0.4	11.1 ± 0.5	4.2 ± 0.4	2.4 ± 0.2	18.4
48.3	14.1 ± 0.5	11.8 ± 0.7	3.9 ± 0.1	2.1 ± 0.2	20.1
51.8	14.9 ± 0.7	12.9 ± 0.7	3.6 ± 0.4	1.8 ± 0.2	21.8
57.5	15.4 ± 0.3	13.4 ± 0.4	3.2 ± 0.4	1.6 ± 0.1	24.7
65.3	15.7 ± 0.3	13.7 ± 0.4	2.8 ± 0.4	1.5 ± 0.1	28.5

[a] In units of rad s^{-1}; uncertainties are one standard deviation from the average of five spectra. [b] Calculated Lorentzian contribution to the observed width. [c] Calculated from least-squares fit of $T_{2,0}^{-1}$ (from Table I) to $1/T$. [d] In units of 10^{-6} s. [e] Computed, using eq 10, from $A_C^D = 4.9 \times 10^5$ Hz and T_{1e} from ESR data.

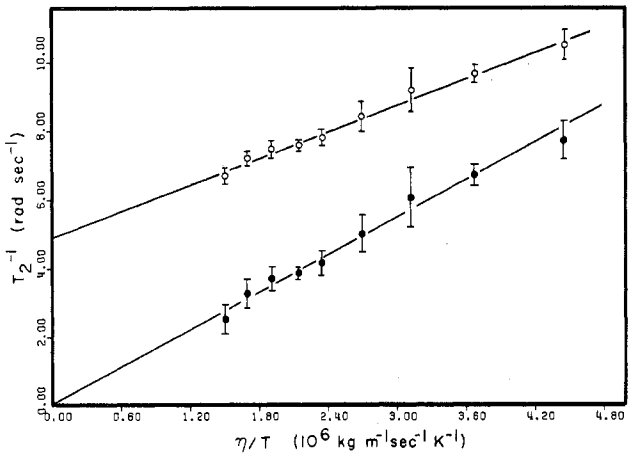

Figure 2. Plot of H NMR line widths vs. η/T for 0.1 M NaOH in D_2O: (○) observed; (●) calculated assuming W_g = 4.45 rad s^{-1}.

line shapes were significantly non-Lorentzian, indicating a broadening contribution from magnetic field inhomogeneity. Assuming that the inhomogeneous broadening can be described by a Gaussian distribution of Lorentzian lines, a procedure was developed to correct the measured line widths; the method is described in the Appendix.[11] Analysis of observed line shapes was not successful in determining a single consistent value of W_g, the Gaussian width, but the attempts pointed to a value of W_g in the range of 2.0–5.6 rad s^{-1}. In order to have a consistent correction scheme, a value of W_g = 4.45 rad s^{-1} was chosen, a value which corrects the D_2O line widths plotted in Figure 2 to give a zero intercept at infinite temperature. This is therefore the maximum consistent correction possible. The same value of W_g was used to correct the ^{2}H magnetic resonance line widths of basic solutions containing vanadium(IV). These corrected values are given in Table II along with the normalized line widths, PT_{2p}^D (P = [metal]/[H_2O]), which are also plotted in Figure 3 as a function of temperature.

^{1}H NMR Line Width Experiments. The observed ^{1}H NMR line widths of solutions containing $VO(OH)_3^-$ were generally much broader than those of metal-free solutions. Since there was no evidence of inhomogeneous broadening in these spectra, no corrections for field inhomogeneity were necessary. The normalized residual broadening, PT_{2p}^H, is plotted in Figures 3 and 4 as a function of reciprocal temperature. The linearity of the plots suggests that T_{2p}^H is dominated by an exchange lifetime contribution. Analysis of the dependence of PT_{2p}^H on hydroxide concentration shown in Figure 4 indicates that the rate law for exchange is

$$\text{rate} = k[VO(OH)_3^-][OH^-] \quad (1)$$

Solutions with NaOH concentrations of less than 0.10 M were

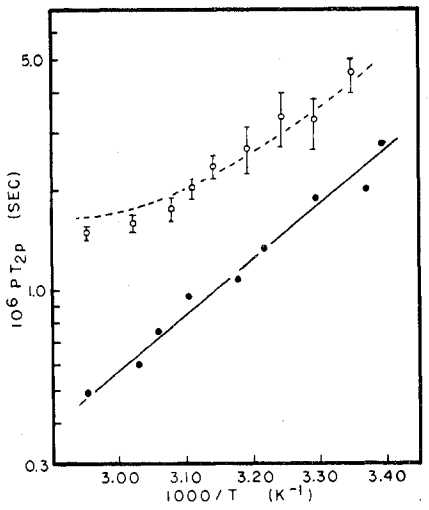

Figure 3. Normalized relaxation times, PT_{2p}^D (○) and PT_{2p}^H (●), vs. inverse temperature; solutions were 0.92 mM $VOSO_4$, 0.1 M NaOH, and 99% D_2O. The dashed curve was calculated from eq 9a.

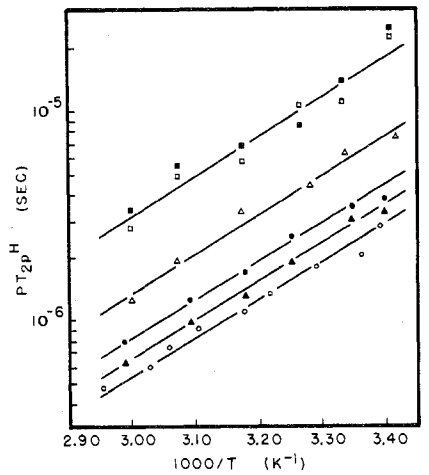

Figure 4. Normalized relaxation times, PT_{2p}^H, vs. inverse temperature for 99% D_2O solutions, 0.92 mM in $VOSO_4$ and 0.02 M NaOH, 0.08 M NaCl (□); 0.02 M NaOH, 0.08 M $NaNO_3$ (■); 0.04 M NaOH, 0.06 M NaCl (△); 0.06 M NaOH, 0.04 M NaCl (●); 0.08 M NaOH, 0.02 M NaCl (▲); and 0.10 M NaOH (○).

maintained at constant 0.10 M ionic strength by addition of NaCl or $NaNO_3$. The results were independent of the choice of anion.

ESR Line Width Experiments. ESR line widths were measured for both the $VO(OD)_3^-$ and $VO(OH)_3^-$ species. The derivative line widths for each hyperfine component were fitted to the power series[2]

$$W_i = \alpha + \beta m_i + \gamma m_i^2 + \delta m_i^3 \quad (2)$$

where m_i is the vanadium nuclear spin quantum number for the ith hyperfine line. Expressions for contributions of motional averaging of the g and hyperfine tensor anisotropies to the parameters α, β, γ, and δ for a molecule of axial symmetry are given by Kivelson et al.[12,13] The rotational correlation time, τ_R, was calculated from γ for each temperature; details of the calculations were given previously.[2]

The experimental and calculated parameters are presented in Tables III and IV. Figure 5 shows that τ_R is linear in η/T, as expected from the Debye equation

$$\tau_R = 4\pi r^3 \eta / 3kT \quad (3)$$

The residual line widths, $\alpha - \alpha'$, are plotted in Figure 6 as a function of τ_R^{-1}. Each line was fitted to the expression $\alpha -$

Table III. ESR Line Width Parameters for $VO(OD)_3(D_2O)_2^-$ [a]

	Exptl				Calcd			
t, °C	α	β	γ	δ	τ_R [b]	α'	β	δ
18.5	14.4 ± 1.8	1.69 ± 0.30	0.95 ± 0.13	−0.04 ± 0.02	5.89	10.79	1.20	−0.013
20.1	12.4 ± 0.7	0.78 ± 0.07	0.52 ± 0.03	−0.015 ± 0.006	3.56	7.65	0.80	−0.008
21.4	12.1 ± 1.0	0.77 ± 0.07	0.51 ± 0.04	−0.005 ± 0.004	3.75	7.63	0.79	−0.008
30.2	11.8 ± 0.7	0.65 ± 0.07	0.39 ± 0.03	−0.006 ± 0.006	2.51	6.81	0.67	−0.007
30.2	11.9 ± 1.0	0.63 ± 0.07	0.40 ± 0.03	−0.002 ± 0.004	2.59	6.90	0.69	−0.007
40.0	11.6 ± 0.6	0.53 ± 0.03	0.30 ± 0.02	−0.002 ± 0.002	1.97	6.14	0.57	−0.006
40.0	11.4 ± 0.8	0.57 ± 0.05	0.29 ± 0.02	−0.005 ± 0.003	1.95	6.11	0.56	−0.006

[a] In units of gauss; uncertainties given are standard deviations. [b] In units of 10^{-11} s.

Table IV. ESR Line Width Parameters for $VO(OH)_3(H_2O)_2^-$ [a]

	Exptl				Calcd			
t, °C	α	β	γ	δ	τ_R [b]	α'	β	δ
8.7	17.4 ± 1.4	1.10 ± 0.13	0.64 ± 0.06	−0.01 ± 0.01	4.03	8.50	0.91	0.010
10.0	16.9 ± 1.0	1.01 ± 0.14	0.61 ± 0.04	−0.02 ± 0.01	3.82	8.26	0.88	−0.009
20.1	16.7 ± 1.4	0.79 ± 0.09	0.49 ± 0.04	−0.009 ± 0.006	3.14	7.51	0.78	−0.008
20.1	16.4 ± 0.8	0.80 ± 0.09	0.45 ± 0.03	−0.013 ± 0.008	2.88	7.22	0.73	−0.008
30.0	16.7 ± 1.3	0.70 ± 0.06	0.31 ± 0.02	−0.014 ± 0.004	2.05	6.25	0.58	−0.006
30.2	16.6 ± 1.1	0.75 ± 0.07	0.32 ± 0.02	−0.020 ± 0.005	2.10	6.32	0.60	−0.006
40.0	16.0 ± 1.1	0.61 ± 0.06	0.25 ± 0.02	−0.009 ± 0.004	1.67	5.70	0.50	−0.005
40.0	16.5 ± 1.1	0.64 ± 0.08	0.23 ± 0.02	−0.012 ± 0.007	1.56	5.51	0.48	−0.005

[a] In units of gauss; uncertainties given are standard deviations. [b] In units of 10^{-11} s.

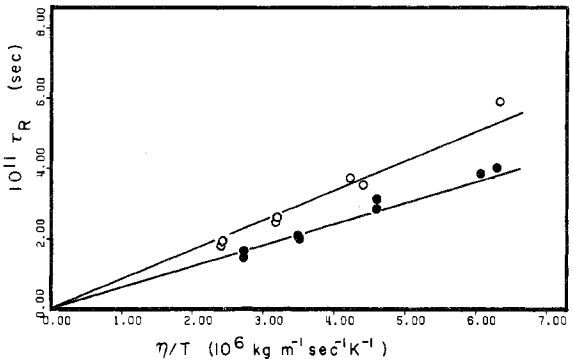

Figure 5. Rotational correlation times calculated from ESR data for $VO(OH)_3(H_2O)_2^-$ (●) and $VO(OD)_3(D_2O)_2^-$ (○) vs. η/T.

$\alpha' = a_0 + a_1\tau_R^{-1}$, where $a_1\tau_R^{-1}$ is related to the spin-rotation contribution to the electron transverse relaxation time, α'', by

$$a_1\tau_R^{-1} = (2h/3^{1/2}g\beta)(T_{2e}^{-1})_{\alpha''} \quad (4)$$

The least-squares parameters for the lines of Figure 6 are the following: for $VO(OH)_3^-$, $a_0 = 7.4 \pm 0.3$ G and $a_1 = (5.5 \pm 0.6) \times 10^{-11}$ G s; for $VO(OD)_3^-$, $a_0 = 3.2 \pm 0.3$ G and $a_1 = (4.4 \pm 0.7) \times 10^{-11}$ G s. The spin-rotational contribution to T_{2e}^{-1} is given by Atkins and Kivelson[14]

$$(T_{2e}^{-1})_{\alpha''} = \tau_R^{-1}(\Delta g_\parallel^2 + 2\Delta g_\perp^2)/9 \quad (5)$$

where $\Delta g_\parallel = g_e - g_\parallel$ and $\Delta g_\perp = g_e - g_\perp$. Using eq 4 and 5, along with the experimental values of $\Delta g_\parallel$ and $\Delta g_\perp$,[1] the value of 2.5×10^{-11} G s is computed for a_1 in satisfactory agreement with the above values obtained from the slopes of Figure 6.

Discussion

Mechanism of the Proton Transfer Reaction. The lower limit on the oxygen residence time in the trihydroxo vanadyl anion was found to be 7×10^{-5} s at 65 °C. Since PT_{2p}^H at this temperature is on the order of 5×10^{-7} s, proton exchange is clearly independent of oxygen exchange. Preliminary analysis of the proton magnetic resonance results showed that hydrogen exchange between $VO(OH)_3(H_2O)_2^-$ and solvent water was first order in hydroxide ion, suggesting that the exchange process involves proton (deuteron) abstraction from the equatorial water molecules of the trihydroxovanadyl

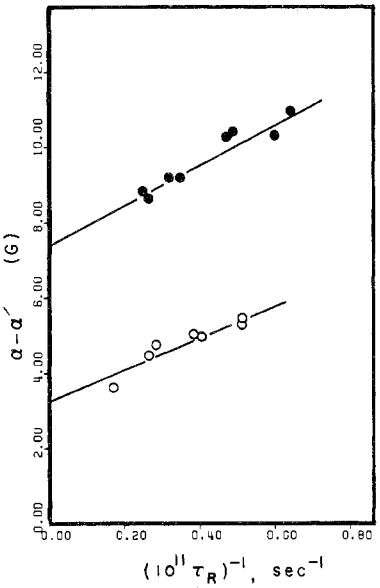

Figure 6. Residual ESR line widths for $VO(OH)_3(H_2O)_2^-$ (●) and $VO(OD)_3(D_2O)_2^-$ (○) as functions of the inverse of the rotational correlation time.

complex by OH^-, followed by rapid protonation of one of the four resulting hydroxo ligands. Since we have no evidence for further ionization of $VO(OH)_3(H_2O)_2^-$ up to pH 14, the equilibrium constant for the reaction

$$VO(OH)_3(H_2O)_2^- + OH^- \underset{k_{-1}}{\overset{k_1}{\rightleftharpoons}} VO(OH)_4(H_2O)^{2-} + H_2O \quad (6)$$

is less than one. If $VO(OH)_4(H_2O)^{2-}$ is a stronger base than OH^-, k_{-1} is expected to be near the diffusion-controlled limit.[15] Since protonation of $VO(OH)_4(H_2O)^{2-}$ could occur at any of the four equatorial hydroxo ligands, proton exchange amounts to rapid averaging of the four equatorial ligands. This mechanism leads to a three-site exchange model which was used for detailed analysis of the line width data.

We assume that bulk water protons (site A), hydroxo ligand protons (site B), and equatorial ligand water protons (site C) are magnetically and kinetically distinguishable. The axial

Table V. Intersite Transition Probabilities[a]

i	j A	B	C
A		0	[M]/2[H_2O]
B	0	$^3/_4$	$^1/_4$
C	$^1/_2$	$^3/_8$	$^1/_8$

[a] The probabilities, given that proton abstraction occurs from $VO(OH)_3(H_2O)_2^-$, that protons originally at site i will end at site j.

water molecule of the vanadyl complex is assumed to exchange very rapidly and to contribute negligibly to the observed line widths.[3] In the forward direction of reaction 6, one of the equatorial water protons becomes a bulk water proton, leaving the other water proton at a hydroxo site. Thus the forward reaction corresponds to simultaneous C → A and C → B transitions. The reverse direction of reaction 6 is presumed to immediately follow; in particular, we assume that the lifetime of the $VO(OH)_4^{2-}$ ion is short compared with nuclear spin relaxation times so that the sequential C → B → C transition would have no effect on the observed relaxation time. In the reverse step, one of the hydroxo ligands is protonated, corresponding to simultaneous A → C and B → C transitions. The probabilities of the various transitions are given in Table V. Thus, if $\tau_m^{-1} = k_1[OH^-]$ is the pseudo-first-order rate constant for reaction 6, the relevant intersite rate constants needed for the modified Bloch equations are found by multiplying τ_m^{-1} by the appropriate transition probabilities from Table V. According to Table V, the probability for an A → C transition is equal to $P/2$, where P = [metal]/[H_2O].

The modified Bloch equations corresponding to the three-site model of Table V were solved by the methods of Swift and Connick;[16] details are given in the Appendix.[11] Defining $z = \tau_m/T_{2C}$ and $R = T_{2C}/T_{2B}$, we have

$$PT_{2p} = 2\tau_m + 2T_{2C}\left(\frac{1+4Rz}{2+3R+8Rz}\right) \quad (7)$$

In order to relate the line widths measured in the ^1H and ^2H NMR experiments, we have used a procedure suggested by Reuben and Fiat[6,17] which utilizes the relation

$$T_{2C}^D/T_{2C}^H = T_{2B}^D/T_{2B}^H \simeq (\gamma_H/\gamma_D)^2 = 42.5 \quad (8)$$

The ^1H and ^2H magnetic resonance line width measurements were performed on solutions which were 99% D_2O. Under these conditions, τ_m should be essentially the same for either nucleus. Using eq 8 to eliminate T_{2C}^H, eq 7 may be written for each nucleus as

$$PT_{2p}^D = 2\tau_m + 2T_{2C}^D\left(\frac{1+4Rz}{2+3R+8Rz}\right) \quad (9a)$$

$$PT_{2p}^H = 2\tau_m + (T_{2C}^D/21.25)\left(\frac{1+170Rz}{2+3R+340Rz}\right) \quad (9b)$$

where $z = \tau_m/T_{2C}^D$.

Several authors have pointed out that the ratio of T_{2C}^D/T_{2C}^H is usually less than 42.5;[18-20] observed ratios generally fall in the range of 10–42[19,20] with a value of 28 ± 9 for $VO(acac)_2$ in deuteriochloroform.[18] However, the ratio differs from 42.5 to the extent that the interaction between the deuterium nuclear quadrupole moment and the electric field gradient of the complex makes an important contribution to T_{2C}^D. For the trihydroxovanadyl ion, the electron–proton (deuteron) isotropic coupling constant is particularly large and should make a much more important contribution to T_{2C}^D than the quadrupolar contribution; the approximation of eq 8 should therefore be a good one.

As indicated by the linear ^1H NMR data of Figure 4, PT_{2p}^H is determined primarily by τ_m over the experimental temperature range. For reasonable values of z and R, the second term of eq 9b is at most comparable in magnitude with $2\tau_m$. Values of τ_m were calculated using the following procedure. The relaxation times, T_{2C}^D, were calculated from

$$T_{2C}^{-1} = (1/3)S(S+1)(2\pi A_C)^2 T_{1e} \quad (10)$$

where T_{1e} is the electron spin–lattice relaxation time, computed from ESR data (see below) and A_C^D is the electron–deuteron hyperfine coupling constant; A_C^D was assumed to be 4.9×10^5 Hz, the value found for the ^2H coupling in an aquo ligand in $VO(D_2O)_5^{2+}$.[21] These T_{2C}^D values, together with values of R ranging from 6 to 20, were used in eq 9b to compute τ_m from PT_{2p}^H. It was found that the results were quite independent of R within that range.

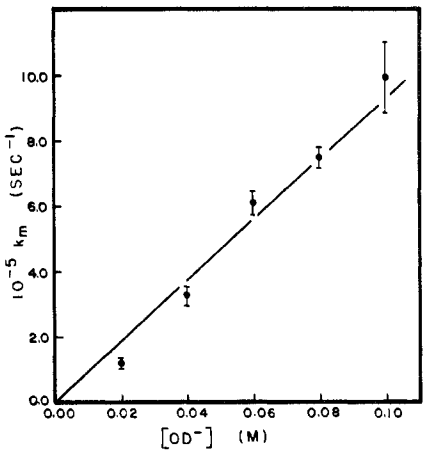

Figure 7. The observed rate constant $k_m = \tau_m^{-1}$ for deuteron exchange as a function of hydroxide concentration at 25 °C for 99% D_2O solutions, 0.92 mM in $VOSO_4$.

The principal contributions to T_{1e} in the case of the vanadyl ion are from the motional averaging of anisotropies in the **g** and hyperfine tensors and from the coupling of the electron spin to the rotational motion of the molecule as a whole

$$T_{1e}^{-1} = (T_{1e}^{-1})_{\alpha'} + (T_{1e}^{-1})_{\alpha''} \quad (11)$$

The motional averaging contributions may be calculated using the nonsecular terms of the equations for $(T_{2e}^{-1})_{\alpha'}$ given by Wilson and Kivelson[12]

$$(T_{1e}^{-1})_{\alpha'} = (g_0\beta_0/45\hbar)^2 u\tau_R(3(\Delta g/g_0)^2 B_0^2 - (\Delta g/g_0)abI(I+1) + (b^2/2)I(I+1)[7-5f(a/B_0)]) \quad (12)$$

where τ_R is the rotational correlation time, g_0 and a are the isotropic g value and vanadium nuclear hyperfine coupling, respectively, $\Delta g = g_\parallel - g_\perp$ and $b = a_\parallel - a_\perp$ are the anisotropies, B_0 is the magnetic field, $u = (1+\omega_0^2\tau_R^2)^{-1}$, $f = \omega_0^2\tau_R^2 u$, and I is the metal nuclear spin quantum number ($^7/_2$ for ^{51}V). In the magnetic field of the NMR experiments, $\omega_0\tau_R > 1$ so that $u\tau_R \simeq uf\tau_R \simeq \omega_0^{-2}\tau_R^{-1}$; $(T_{1e}^{-1})_{\alpha'}$ is expected to increase with τ_R^{-1} and thus with T/η (see eq 3). The spin–rotational contributions to T_{1e} and T_{2e} are identical[22] so that $(T_{1e}^{-1})_{\alpha''}$ was calculated from a_1, the slope of the plot of $(\alpha - \alpha')$ vs. τ_R^{-1} for the D_2O data of Figure 6. $(T_{1e}^{-1})_{\alpha''}$ is linear in τ_R^{-1} and so should also increase with η/T; thus T_{2C}^D is expected to increase with increasing temperature.

Values of τ_m at 25 °C were interpolated from the data at each NaOH concentration and are shown in Figure 7 as a function of [OH^-]. The plot shows that the [OH^-] = 0 intercept is zero within experimental error, confirming the assumed rate law, eq 1. Application of the Eyring equation to $k_1 = \tau_m^{-1}/[OH^-]$, using all the available data—39 values at temperatures ranging from 10 to 65 °C and [OH^-] = 0.02–0.10 M—resulted in the activation parameters presented in Table VI.

Table VI. Rate Constants and Activation Parameters for Proton Exchange Reactions

Species	k^a	$\Delta H^{\ddagger}$ [b]	$\Delta S^{\ddagger}$ [c]	Ref
$VO(OD)_3(D_2O)_2^-$	8.4 [OD^-]	40 ± 2	22 ± 7	This work
$VO(H_2O)_5^{2+}$	1.8 [H^+]	10	−92	6
	1.6 [H^+]	11	−89	23
$Cr(H_2O)_6^{3+}$	0.48 [H^+]	0	−138	23
$CrCl(H_2O)_5^{2+}$	1.3 [H^+]	4	−106	23
$VO(H_2O)_5^{2+}$	0.48 [CH_3COOH]	34	−27	23
$Cr(H_2O)_6^{3+}$	1.7 [CH_3COOH]	13	−105	23
$CrCl(H_2O)_5^{2+}$	0.23 [CH_3COOH]	27	−71	23
$VO(H_2O)_5^{2+}$	0.062	50	14	6
	0.10	33	−37	24
$Cr(H_2O)_6^{3+}$	1.7	47	32	5
	1.2	25	−44	24
$CrCl(H_2O)_5^{2+}$	0.57	16	−89	24
$Al(H_2O)_6^{3+}$	0.079	54	32	26
$CrOH(H_2O)_5^{2+}$	8.5			5
$Pt(NH_2)(NH_3)_5^{3+}$	220	3	−75	4

[a] Pseudo-first-order rate constant at 25 °C; units of 10^6 s^{-1}. [b] In units of kJ mol^{-1}. [c] In units of J mol^{-1} K^{-1}.

Several mechanisms have been suggested for proton exchange between coordinated ligands and solvent water. Swift and co-workers[23,24] have pointed out that proton exchange processes must in general follow a three-step mechanism involving (i) encounter of the reacting partners, (ii) rearrangement of the encounter complex to a hydrogen-bonded complex, and (iii) proton transfer within the hydrogen-bonded complex. If step i is not rate limiting, the entropy of activation is expected to be governed primarily by the structure of the hydrogen-bonded complex; the enthalpy of activation should be associated with the proton transfer step itself and might be expected to increase with $-\Delta pK_{\alpha}$.[25]

Catalysis of proton exchange between coordinated water and bulk water by both strong and weak acids has been observed for $VO(H_2O)_5^{2+}$,[6,23] $Cr(H_2O)_6^{3+}$,[23] $CrCl(H_2O)_5^{2+}$,[23] and $Ni(H_2O)_6^{2+}$.[23] Activation parameters for several of the reactions are given in Table VI. Swift has suggested that catalysis by strong acids differs from catalysis by weak acids (e.g., acetic acid) in the structures of the hydrogen-bonded complexes; structures I and II were postulated for the two cases,

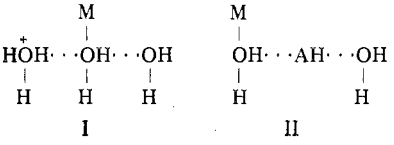

I II

respectively.[23] Both structures involve two hydrogen bonds although the steric requirements of structures I are somewhat more stringent. Catalysis by strong acids is thus expected to involve near-zero enthalpies of activation and large negative entropies while catalysis by weak acids is expected to show significant enthalpies of activation and less negative entropies.

A third type of mechanism has been postulated by Grunwald and Fong[4] for solvent proton exchange with $Pt(NH_2)(NH_3)_5^{3+}$ and by Melton and Pollack[5] for exchange with $Cr(OH)(H_2O)_5^{2+}$. Proton exchange with these bifunctional species is thought to involve cyclic hydrogen-bonded complexes as shown in structures III. Activation parameters were not

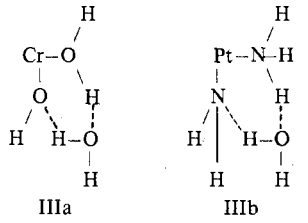

IIIa IIIb

measured for $Cr(OH)(H_2O)_5^{2+}$, but as seen in Table VI, exchange is fast in both cases and $Pt(NH_2)(NH_3)_5^{3+}$ shows the expected small enthalpy of activation and large negative entropy.

Direct proton transfer from coordinated water to bulk water has been observed for $VO(H_2O)_5^{2+}$,[6,24] $Cr(H_2O)_6^{3+}$,[5,24] $CrCl(H_2O)_5^{2+}$,[24] and $Al(H_2O)_6^{3+}$.[26] Apparently because of the difficulty of separating the uncatalyzed and H^+-catalyzed rate contributions, agreement between independently measured activation parameters for the uncatalyzed path is poor. Nonetheless, the activation enthalpies listed in Table VI are seen to be considerably larger than those for the corresponding H^+-catalyzed reactions and activation entropies are positive or at least less negative than for the H^+-catalyzed reactions. If, as has been shown to be the case for Al^{3+},[26] proton transfer involves a hydrogen-bonded complex such as structure IV and

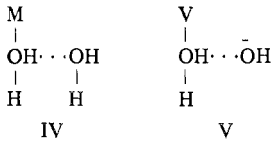

IV V

a shift along a single hydrogen bond, the entropy of activation would be expected to be nearer zero and the enthalpy related to the pK_a of the coordinated water protons.

These results seem consistent with the mechanism proposed for solvent proton exchange with $VO(OH)_3(H_2O)_2^-$ which involves the hydrogen-bonded complex shown in structures V. The activation enthalpy of 40 kJ mol^{-1} for proton transfer to the strong base OH^- suggests that the equatorial water protons of $VO(OH)_3(H_2O)_2^-$ are very weakly acidic and that proton transfer directly to water is energetically prohibitive.

It remains somewhat surprising that $VO(OH)_3(H_2O)_2^-$ does not undergo proton exchange with solvent water via a bifunctional mechanism. An upper limit on the base-independent rate constant is about 4×10^4 s^{-1} at 25 °C, several orders of magnitude slower than observed for $Cr(OH)(H_2O)_5^{2+}$ and $Pt(NH_2)(NH_3)_5^{3+}$.

The substitution of anionic ligands for aquo ligands in vanadyl complexes has been observed to increase the rate of exchange of the remaining coordinated water. Thus in vanadyl complexes with iminodiacetic acid and sulfosalicylic acid,[27] as well as in the dichloro[28] and the dihydrogenphosphato[29] complexes, oxygen exchange is faster than in the aquo cation. No such effect was observed in this study, presumably because rapid hydrogen exchange effectively averages the four equatorial oxygen ligands on the time scale defined by oxygen exchange. Thus, for times longer than about 10^{-5} s (at 25 °C in 0.1 M NaOH), the four equatorial V–O bonds are all somewhat stronger and more covalent than those in the pentaaquo cation, resulting in the slower exchange of oxygen atoms in the trihydroxovanadyl ion.

Relaxation Results. In our previous work on the ESR line widths of $VO(OH)_3(H_2O)_2^-$,[2] the difference in residual widths measured for H_2O and D_2O solutions, $(\alpha - \alpha')^H - (\alpha - \alpha')^D$, was attributed to unresolved hyperfine coupling of the ligand protons. The results of the present work, where both H_2O and D_2O solutions were studied as a function of temperature, are consistent with the earlier conclusion. The slopes of the plots of $\alpha - \alpha'$ vs. τ_R^{-1} in Figure 6 are equal within experimental error, showing that the additional broadening in the H_2O solution is temperature independent. Furthermore, line shape simulations which included the kinetics of proton exchange showed that proton exchange makes an entirely negligible contribution to ESR line widths.

Line shape simulations similar to those described previously[2] suggest that an average proton coupling, $\langle a \rangle = (2a^C + 3a^B)/5$, of 3–4 G is required to explain the difference in the H_2O and D_2O results, in general agreement with the previous estimate of 4.5 G.[2] It is impossible to determine the average coupling precisely, however, in part because of accuracy limitations

inherent in the data but also because the results are somewhat sensitive to the ratio of hydroxo to aquo proton coupling constants, a^B/a^C. If we assume a coupling of 1.1 G for the aquo protons (the value found for $VO(H_2O)_5^{2+}$)[21] then the hydroxo proton coupling which best fits the line width data is about 4.4 G, corresponding to an average coupling of 3.1 G.

The ^2H NMR line widths provide an independent check on the conclusions drawn from the ^1H NMR and ESR experiments. Equation 9a can be used to calculate the ^2H normalized line widths, PT_{2p}^D, from τ_m and T_{2C}^D, data entirely independent of the ^2H NMR results. Values of τ_m were obtained from the ^1H NMR data as described above; values of T_{2C}^D were computed from the ESR data and the assumption that $A_C^D = 4.9 \times 10^5$ Hz and are given in Table II. PT_{2p}^D was computed for various assumed values of R ranging from 1 to 20. The best overall fit was for $R = 16$, corresponding to $A^B/A^C = 4.0$, in remarkable agreement with the virtually identical conclusion reached from the ESR line width analysis. Furthermore, the normalized widths obtained for $R = 16$ are plotted as the dashed curve of Figure 3 and are seen to be in excellent agreement with the experimental values. The success in predicting the ^2H normalized widths, while probably not absolutely conclusive, does give us considerably greater confidence in the procedures used to obtain the rate constants and in the conclusions reached regarding the ligand proton hyperfine coupling.

Acknowledgment. Helpful discussions with J. O. Edwards, M. J. Kaus, and R. G. Lawler are greatly appreciated. This work was supported in part by a grant from the National Institute of Environmental Health Sciences.

Registry No. $VO(OH)_3(H_2O)_2^-$, 56586-21-1.

Supplementary Material Available: A derivation of eq 7 and the procedure for corrections of inhomogeneously broadened lines (5 pages). Ordering information is given on any current masthead page.

References and Notes

(1) M. M. Iannuzzi and P. H. Rieger, *Inorg. Chem.*, **14**, 2895 (1975).
(2) M. M. Iannuzzi, C. P. Kubiak, and P. H. Rieger, *J. Phys. Chem.*, **80**, 541 (1976).
(3) J. Reuben and D. Fiat, *Inorg. Chem.*, **6**, 579 (1967); K. Wüthrich and R. E. Connick, *ibid.*, **6**, 583 (1967).
(4) E. Grunwald and D.-W. Fong, *J. Am. Chem. Soc.*, **94**, 7371 (1972).
(5) B. F. Melton and V. L. Pollack, *J. Phys. Chem.*, **73**, 3669 (1969).
(6) J. Reuben and D. Fiat, *J. Am. Chem. Soc.*, **91**, 4652 (1969).
(7) R. R. Reeder and P. H. Rieger, *Inorg. Chem.*, **10**, 1258 (1971).
(8) A. L. Van Geet, *Anal. Chem.*, **42**, 679 (1970).
(9) The results of the ESR intensity vs. [V(IV)] experiment reported in ref 1 are in error by a factor of 10; ESR intensity was linear in [V(IV)] up to about 1.5 mM.
(10) C. Weiske, Dissertation, Technischen Universität Berlin, 1960.
(11) Supplementary material.
(12) R. Wilson and D. Kivelson, *J. Chem. Phys.*, **44**, 154 (1966).
(13) D. Kivelson, *J. Chem. Phys.*, **33**, 1094 (1960).
(14) P. W. Atkins and D. Kivelson, *J. Chem. Phys.*, **44**, 169 (1966).
(15) M. Eigen, W. Kruse, G. Maas, and L. De Maeyer, *Prog. React. Kinet.*, **2**, 285 (1964).
(16) T. J. Swift and R. E. Connick, *J. Chem. Phys.*, **37**, 307 (1962).
(17) J. Reuben and D. Fiat, *J. Am. Chem. Soc.*, **91**, 1242 (1969).
(18) B. M. Fung, *J. Chem. Phys.*, **58**, 192 (1972).
(19) A. Johnson and G. W. Everett, Jr., *J. Am. Chem. Soc.*, **94**, 1419 (1972).
(20) G. W. Everett, Jr., and A. Johnson, *J. Am. Chem. Soc.*, **94**, 6398 (1972).
(21) J. Reuben and D. Fiat, *Inorg. Chem.*, **8**, 1821 (1969).
(22) P. S. Hubbard, *Phys. Rev.*, **131**, 1155 (1963).
(23) T. A. Stephenson, T. J. Swift, and J. B. Spencer, *J. Am. Chem. Soc.*, **90**, 4291 (1968).
(24) T. J. Swift, T. A. Stephenson, and G. R. Stein, *J. Am. Chem. Soc.*, **89**, 1611 (1967).
(25) R. P. Bell, "The Proton in Chemistry", Cornell University Press, Ithaca, N.Y., 1973, p 194.
(26) D.-W. Fong and E. Grunwald, *J. Am. Chem. Soc.*, **91**, 2413 (1969).
(27) K. Wüthrich and R. E. Connick, *Inorg. Chem.*, **7**, 1377 (1968).
(28) A. H. Zeltmann and L. O. Morgan, *Inorg. Chem.*, **10**, 2739 (1971).
(29) M. W. Kendig and P. H. Rieger, *Inorg. Chim. Acta*, **17**, 175 (1976).

Contribution No. 5405 from the Arthur Amos Noyes Laboratory of Chemical Physics, California Institute of Technology, Pasadena, California 91125

Fluorine and Alkyl Substituent Effects on the Gas-Phase Lewis Acidities of Boranes by Ion Cyclotron Resonance Spectroscopy

M. K. MURPHY and J. L. BEAUCHAMP*[1]

Received May 23, 1977 AIC703773

Formation of Lewis acid–base adducts R_3BF^- and R_2FBF^- in reactions of SF_5^- and SF_6^- with neutral boranes R_3B (R = CH_3, C_2H_5, i-C_3H_7, and F) is examined using trapped-ion cyclotron resonance techniques. Fluoride transfer reactions observed in binary mixtures of the various boranes (in the presence of traces of SF_6 acting as the source of F^-) establish the Lewis acidity order $BF_3 > (i\text{-}C_3H_7)_2FB > (i\text{-}C_3H_7)_3B > (C_2H_5)_2FB > (C_2H_5)_3B > (CH_3)_2FB > (CH_3)_3B > SF_4$ in the gas phase with F^- as reference base. Quantitative estimates of adduct bond dissociation energies $D[R_3B\text{–}F^-]$ and heats of formation of adducts R_3BF^- are derived. Variations in Lewis acidity resulting from alkyl and fluoro substitution on boron are discussed in terms of properties characteristic of substituents and the anion reference base.

Introduction

The general concepts of electron-pair donor–acceptor chemistry, formalized in the Lewis definition of acids and bases,[2] have contributed much to understanding relationships between molecular structure and chemical reactivity important in organic, inorganic, and organometallic chemistry. Investigations of acid A and base B transfer processes (reactions 1 and 2, respectively) can yield direct measurements of the

$$AB_1 + B_2 \rightarrow B_1 + AB_2 \qquad \Delta H = D[B_1\text{-A}] - D[B_2\text{-A}] \qquad (1)$$

$$A_1B + A_2 \rightarrow A_1 + A_2B \qquad \Delta H = D[A_1\text{-B}] - D[A_2\text{-B}] \qquad (2)$$

bond energies D[A–B] and provide a methodology suitable for the study of factors determining the strengths of acid–base interactions.

Ion cyclotron resonance mass spectrometry (ICR) has proven to be a versatile tool for the study of acid–base reactions[3-5] in the gas phase, in the absence of solvation effects, specifically reactions 1 and 2 where species A and/or B are charged. Recent investigations[6-8] of reactions 1, involving cationic Lewis acids (e.g., Li^+,[6] NO^+,[7] c-$C_5H_5Ni^+$[8]) and various neutral organic and inorganic bases, have yielded insight into the factors governing intrinsic n- and π-donor basicity. Transfer reactions such as eq 2 involving closed shell anionic bases (e.g., H^-, F^-, Br^-) and cations R_3M^+ (where M = C, Si; R = H, alkyl, F) have been exploited for the de-